A Letters Journal Exploring the Frontiers of Physics

October 2008

EPL, **84** (2008) 16002
doi: 10.1209/0295-5075/84/16002

www.epljournal.org

Electrorheological effect and non-Newtonian behavior of a homogeneous nematic cell under shear flow: Hysteresis, bistability, and directional response

J. C. Medina and Carlos I. Mendoza[a]

Instituto de Investigaciones en Materiales, Universidad Nacional Autónoma de México - Apdo. Postal 70-360, 04510 México, D.F., Mexico

received 2 May 2008; accepted in final form 18 August 2008
published online 19 September 2008

PACS 61.30.Gd – Orientational order of liquid crystals; electric and magnetic field effects on order
PACS 47.57.Lj – Flows of liquid crystals
PACS 47.57.Qk – Rheological aspects

Abstract – We study the flow of a homogeneous nematic cell under the simultaneous action of an applied electric field and an applied shear flow. Using a hydrodynamic model that describes the response of a flow-aligning nematic liquid crystal (5CB) we obtain the director's configuration and the velocity profile at the steady states. From these results we construct a phase diagram in the electric field *vs.* shear flow space that displays regions for which the system may have different steady-state configurations of the director's field. The selection of a given steady-state configuration depends on the history of the sample. Due to the competition between shear flow and electric field, the system's viscosity shows a complex non-Newtonian response with regions of shear thickening and thinning. Interestingly, as a consequence of the hysteresis of the system, this response may be asymmetric with respect to the direction of the shear flow. The results also show a moderate electrorheological effect which is also dependent on the history of the sample.

Introduction. – Nematic liquid crystals exhibit interesting flow phenomena due to its non-Newtonian behavior originated by the coupling between the local molecular orientation and the velocity field [1–3]. Although some of these properties have been known for a long time, a large amount of theoretical, numerical and experimental work has been produced in recent years. In particular, a number of publications treat the behavior of nematic liquid crystals in shear and Poiseuille flow fields [4–12].

On the other hand, it has been shown that the influence of an electric field strongly modifies the rheology of liquid crystals [11,12]. This has considerable interest due to its possible application in microsystems [13] since homogeneous fluids, like liquid crystals, present some advantages over conventional electrorheological fluids. Among them, we can mention that liquid crystals, in contrast to other active fluids, do not contain suspended particles. This homogeneity is of particular importance for microsystems since small channels are easily obstructed by suspended particles. Also, they prevent agglomeration, sedimentation and abrasion problems [13]. The electrorheological properties and the static and dynamic flow characteristics of liquid crystals under different conditions have been treated in several papers [13–19].

The purpose of the present work is to study theoretically the steady-state characteristics of a homogeneous cell under the simultaneous action of a shear flow and a perpendicularly applied low-frequency electric field. In spite of the large amount of work done for this and related systems, there are important issues that remain open. Among them, the possibility of multiple steady-state solutions has rarely been considered. For example, in ref. [1] two different director configurations for steady-state Poiseuille flow in a homeotropic cell it is predicted. Also, in ref. [3] this possibility is not excluded for the case of a hybrid nematic cell under shear flow. Here we show that it is possible to construct a phase diagram in the electric field *vs.* shear flow space which contains regions for which multiple steady-state solutions exist and that the choice between the different solutions depends on the history of the sample. We also show that this history-dependent response affects the complex non-Newtonian behavior of the system that becomes dependent on the direction of the shear stress.

[a]E-mail: cmendoza@iim.unam.mx

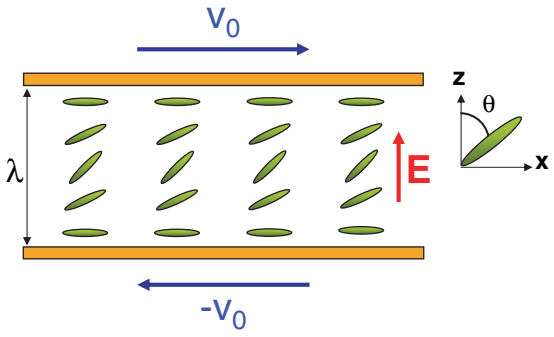

Fig. 1: Schematics of a homogeneous cell subjected to a normal electric field and an applied shear flow.

Model and governing equations. – The system under study consists of a thermotropic nematic layer of thickness l confined between two parallel plates, as depicted in fig. 1. The transverse dimensions, L, of the cell are large compared to l and the cell is under the action of a perpendicular low-frequency electric field. Additionally, the plates may move in opposite directions, each one with speed v_0, producing a shear flow in the (x,z)-plane and along the x-axis. The velocity profile may then be written as $\mathbf{v}=(v_x,0,0)$ (see fig. 1).

The orientational angle, $\theta(\varsigma)$, defined with respect to the z-axis satisfies strong anchoring conditions at the plates

$$\theta(\varsigma=\pm 1/2)=\pi/2, \tag{1}$$

and the only relevant component of the velocity field, v_x, satisfies the non-slip boundary conditions

$$\widetilde{v}_x(\varsigma=\pm 1/2)=\pm\mathrm{sgn}(v_0), \tag{2}$$

where we have defined the normalized variables $\varsigma\equiv z/l$ and $\widetilde{v}_x\equiv v_x/|v_0|$, and $\mathrm{sgn}(x)$ represents the sign function.

Using the common approach of describing the flow of rod-shaped LCs with the theory of Ericksen, Leslie and Parodi (ELP) [20] it is possible to show that the equations that governs the steady state of the system are

$$0=\left(\sin^2\theta+\kappa\cos^2\theta\right)\frac{\mathrm{d}^2\theta}{\mathrm{d}\varsigma^2}+(1-\kappa)\sin\theta\cos\theta\left(\frac{\mathrm{d}\theta}{\mathrm{d}\varsigma}\right)^2$$
$$-\frac{\varepsilon_a\varepsilon_0}{2K_1}l^2E^2\sin(2\theta)+\frac{l\,|v_0|}{K_1}\left(\alpha_3\sin^2\theta-\alpha_2\cos^2\theta\right)\frac{\mathrm{d}\widetilde{v}_x}{\mathrm{d}\varsigma}, \tag{3}$$

$$\frac{\mathrm{d}\widetilde{v}_x}{\mathrm{d}\varsigma}=\mathrm{sgn}(v_0)\,\frac{c(q,m)}{\eta(\theta)}. \tag{4}$$

The first equation reflects the equilibrium of torques on a given element of fluid while the second is the momentum conservation equation. Here, α_i are the Leslie viscosities and $\kappa\equiv K_3/K_1$ with K_1 and K_3 the splay and bend elastic constants of the LC. In eq. (4) $c(q,m)$ is a positive constant that depends only on the electric field and the shear rate and is given by

$$c(q,m)=\frac{2}{\int_{-1/2}^{1/2}\frac{\mathrm{d}\varsigma'}{\eta[\theta(\varsigma')]}}, \tag{5}$$

where

$$\eta(\theta)=\alpha_1\sin^2\theta\cos^2\theta+\eta_b\sin^2\theta+\eta_c\cos^2\theta, \tag{6}$$

is the position dependent viscosity of the LC. In this equation, $\eta_b=(\alpha_3+\alpha_4+\alpha_6)/2$ and $\eta_c=(\alpha_4+\alpha_5-\alpha_2)/2$ are two of the three Miesowicz viscosities [21].

Substituting eq. (4) in eq. (3), we obtain

$$0=\left(\sin^2\theta+\kappa\cos^2\theta\right)\frac{\mathrm{d}^2\theta}{\mathrm{d}\varsigma^2}+(1-\kappa)\sin\theta\cos\theta\left(\frac{\mathrm{d}\theta}{\mathrm{d}\varsigma}\right)^2$$
$$-q\sin(2\theta)+\frac{m}{\eta(\theta)}\left(\alpha_3\sin^2\theta-\alpha_2\cos^2\theta\right), \tag{7}$$

where we have defined a dimensionless field strength

$$q\equiv\frac{\varepsilon_a\varepsilon_0}{2K_1}l^2E^2, \tag{8}$$

and the dimensionless shear rate

$$m\equiv\frac{lv_0c(q,m)}{K_1}. \tag{9}$$

Notice that q takes only positive values, while m is positive if the upper plate of the cell moves to the right and negative if it moves to the left (see fig. 1). Also, note that m and v_0 are not linearly related due to the factor $c(q,m)$. The stationary configuration of the nematic's director can be found by solving eq. (7) numerically using the "shooting" method [22].

Results. – In what follows, the calculations are performed for 4′-n-pentyl-4-cyanobiphenyl (5CB), a flow-aligning LC whose Leslie coefficients at $T=25\,^\circ$C are: $\alpha_1=-0.0060\,$Pa s, $\alpha_2=-0.0812\,$Pa s, $\alpha_3=-0.0036\,$Pa s, $\alpha_4=0.0652\,$Pa s, $\alpha_5=0.0640\,$Pa s, and $\alpha_6=-0.0208\,$Pa s; and the splay and bend elastic constants are $K_1=12\,$pN and $K_3=1.316K_1$, respectively.

Let us first consider the orientational profile. In fig. 2a we plot the orientational angle θ *vs.* the position in the cell ς, as obtained from eq. (7) for various values of the field strength q. In the absence of flow ($m=0$), we recover the usual Frederiks transition in which the molecules are reoriented only for electric field intensities larger than a critical value q_F. Once this threshold is surpassed, we observe that θ decreases with increasing values of q. This is in agreement with the tendency of the molecules to be aligned with the direction of the electric field. Actually, there are two possible steady-state configurations of the director's field, one being the specular reflection of the other with respect to the z-axis. In contrast, once a shear flow is present ($m\neq 0$), the molecules are reoriented for any value of the electric field as shown in fig. 2b. What is more interesting is that there exist combinations of values for the electric field and the applied shear flow for which there are more than one stationary configuration of the director's field. Additionally, in this case the stationary solutions are not the specular reflection of each other. In fig. 2b we

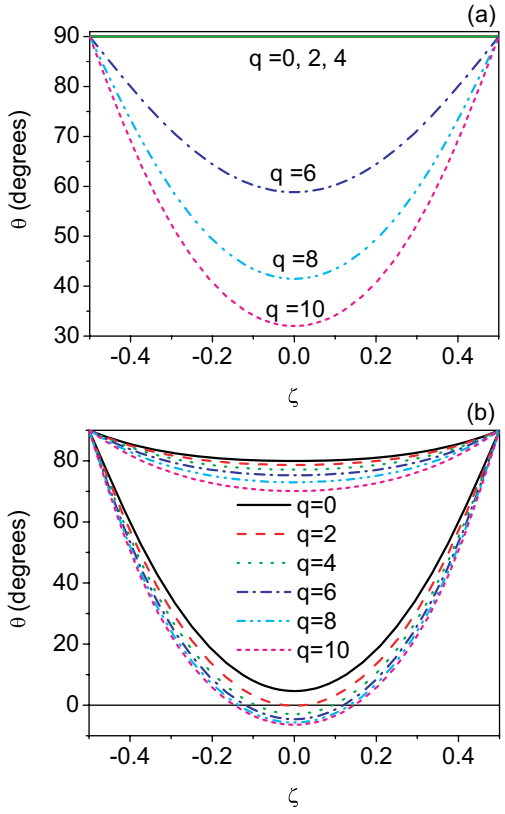

Fig. 2: Nematic's configuration θ as a function of ς for 5CB at $T = 25\,^{\circ}$C. (a) $m = 0$ and (b) $m = 20$. In the latter case two sets of solutions are shown. For the second set we plot $180^{\circ} - \theta$ instead of θ.

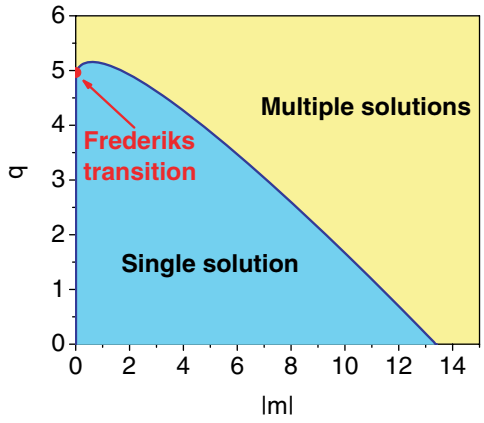

Fig. 3: Phase diagram in the q *vs.* m space showing regions with only one or several steady-state configurations.

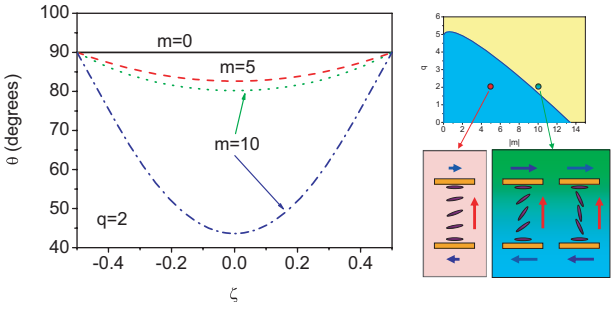

Fig. 4: Nematic's configuration θ as a function of ς for $q = 2$ and different values of m. For the more inclined solution with $m = 10$ we plot $180^{\circ} - \theta$ instead of θ. The upper right panel shows the position in the phase space of the parameters q and m considered. Also, the lower panels show a sketch of the corresponding nematic's steady-state configurations.

have plotted two solutions for each set of parameters, one set of solutions corresponds to configurations much more vertically aligned than the others. The first set of solutions, the ones that are less inclined, are tilted in the opposite direction that the second set, which are more inclined, except for the small region with negative θ near the center of the cell. Note that in order to plot the two sets of solutions in the same graphic, we plot $180^{\circ} - \theta$ for the second set. The origin of the negative region is easy to understand. Let us suppose that under the action of the electric field the molecules will orient with a tilt that conflicts the one the flow acting alone would produce. Then, if we increase the flow, the molecules near the center of the cell will try to adopt the tilt induced by the flow. If the flow is large enough then the molecules near the center of the cell may exceed the vertical position an adopt the right tilt which is given by the negative part of the curves in fig. 2b. The solutions that are less inclined are the continuation of the corresponding to the single solution region as will be explained in more detail in fig. 6. A phase diagram in the q *vs.* m plane that displays regions with one or multiple configurations can be constructed, as shown in fig. 3.

This figure shows the usual Frederiks transition for zero shear flow ($m = 0$) which separates the low electric-field region ($q < q_F$) in which there is no reorientation of the director, from the high electric field region ($q > q_F$) for which the director's field is reoriented in two possible configurations each one being the specular reflection of the other. The phase diagram shows that this transition can be extended to the case in which there is shear flow albeit in this case, there is reorientation of the director field for all values of q and the multiple solutions are not specular reflections of each other. Notice also that for high enough shear rates, the single valuated region disappears and multiple solutions appear for all values of q. In order to understand more clearly the meaning of these regions, in fig. 4 we have plotted the stationary solutions of θ *vs.* ς, for a given value of q and different values of m. In the specific example shown, for $q = 2$ there is a unique solution when $m = 0$ and $m = 5$. However, for $m = 10$, there are two steady-state configurations. One of the two stationary solutions corresponds to a configuration in which the molecules are tilted to the left, which is the tilt direction that the flow would impose in the absence of the electric field. In the other solution, the molecules are tilted to the right, contrary to the tendency

imposed by the flow acting alone. These configurations are schematically shown in the right panel of fig. 4 together with their position in the phase space. Note again that for the second solution for $m = 10$ we have plotted $180° - \theta$. The question of how to set up these different stationary configurations rises naturally. Actually, the selection of one of the configurations over the other depends on the history of the sample as will be discussed below. Let us remark that the solutions we have plotted are the ones that are real stable states. The solutions corresponding to the single-solution region are always stable and continue into the multiple-solutions region. The new solutions in this region appear always in pairs, one of them is unstable (not plotted) and the other locally stable. Which of the stable solutions in this region will be preferred will depend on the conditions of the experiment. Note, however, that the other solution can exist as a metastable state. We have verified that no significant change of the results occurs when we include a pretilt parallel or antiparallel in the boundary conditions. Therefore our results are robust with respect to the presence of a pretilt. Additional crossover lines can be drawn in fig. 3 which separates regions with two, four, and more stable states but these appear for very strong shears and for clarity are not drawn. The fact that the system presents at least two different stable or metastable liquid crystal alignments leads to think of the possibility of switching between these states and use this fact as a mean to produce bistable or multistable devices that could be useful for applications.

Once $\theta(\varsigma)$ has been determined numerically, the velocity profile of the nematic can be obtained integrating eq. (4) taking into consideration the non-slip boundary conditions given by eq. (2) to obtain

$$\widetilde{v}_x(\varsigma) = -\mathrm{sgn}(v_0)\left\{1 - 2\frac{\int_{-1/2}^{\varsigma} \frac{\mathrm{d}\varsigma'}{\eta[\theta(\varsigma')]}}{\int_{-1/2}^{1/2} \frac{\mathrm{d}\varsigma'}{\eta[\theta(\varsigma')]}}\right\}. \qquad (10)$$

As shown in fig. 5 the velocity profile departs from the isotropic Newtonian behavior and this departure is more pronounced for the configurations in which the molecules are tilted in the opposite direction as the one imposed by the flow acting alone. The profile of the curves is symmetrical with respect to the plane that crosses the cell at its middle point. Panel (a) corresponds to the set of solutions that are only slightly reoriented while panel (b) corresponds to the set of solutions that are more vertically aligned.

The practical problem of how to set up the different stationary configurations is exemplified in fig. 6. For clarity, in this figure we have recasted the phase diagram drawing the positive and negative parts of the m-axis and we consider two different processes. In first place, let us suppose that we have the system flowing with a positive shear flow and no applied electric field as indicated by the point A of the phase diagram (see fig. 6). In this situation the system adopts its only possible configuration which is therefore determined by the direction of the flow.

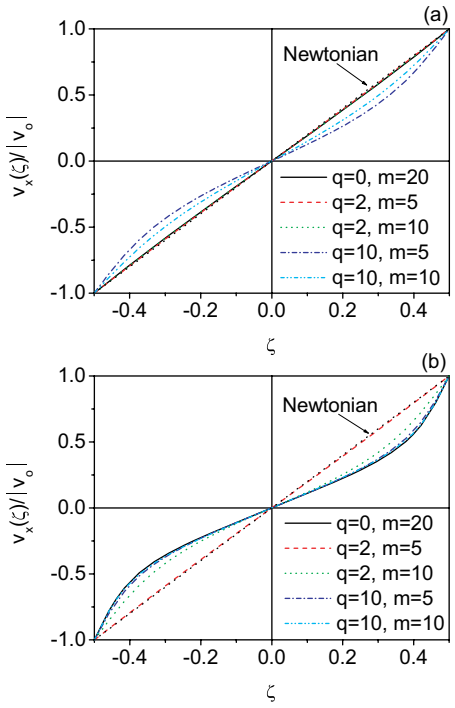

Fig. 5: Velocity profiles $\widetilde{v}_x$ *vs.* ς for different values of q and m. Panel (a) corresponds to the set of solutions in which the director is only slightly reoriented with the application of the electric field while panel (b) corresponds to solutions in which the director is strongly reoriented with q.

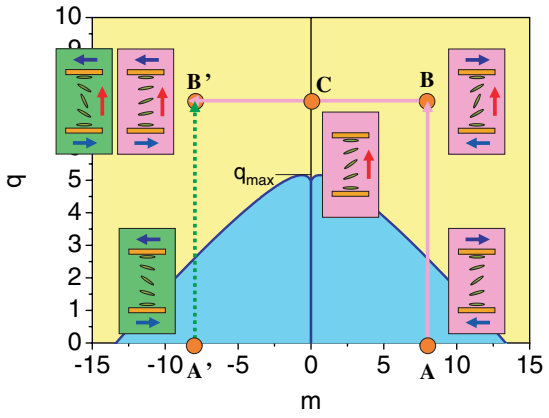

Fig. 6: Sketch of two possible trajectories in the phase diagram that gives rise to two different steady states for a given pair q, m.

Then, one applies gradually an increasing electric field until reaching point B. The electric field tends to align the molecules towards the z-axis but maintaining the tilt direction established previously by the flow at point A. If one now gradually decreases the flow, the system will eventually be located at point C with a configuration whose tilt sense is the same of that of the previous states of the system as indicated by the drawings in fig. 6. Finally, we increase gradually the flow until reaching the same magnitude as in point B but with the opposite direction.

The system is then located in its final state indicated by point B'. During this part of the process, the flow is trying to tilt the molecules in the opposite direction as the one it had previously. However, if the electric field is larger than $q_{\max}$ then the flow cannot overcome the original tilt and the system adopts a configuration as the one sketched at point B' in fig. 6. Note that this final configuration does not correspond to the specular reflection of the one at point B. If on the other hand, we start the whole process at point A' then the system will adopt there its only stationary configuration which is the specular reflection with respect to the z-axis of the corresponding one at point A. Increasing gradually the electric field until reaching point B' the configuration adopted by the system at that point will be the specular reflection of the corresponding configuration at point B, which is therefore different from the configuration adopted by the system at that same point (B') for the first process. Thus, the final configuration of the system for the same set of parameters q and m depends on the history of the sample. It is also possible to switch from one configuration to the other by simply turning off and on the electric field. For example, if the system is at point B' with the alignment produced by the first process explained above, then, turning off and then turning on the electric field will switch the system to the second configuration at B'. To switch again to the first configuration (more precisely, to switch to the specular image of the first configuration) it is necessary to reverse the flow.

The procedure described in the previous paragraph to set up the different stationary configurations may be used to induce a directional response of the system. This can be seen if we consider the trajectory BB' of fig. 6. Starting from point B, a slow oscillatory movement of the plates of the cell will go from B to C to B', then back to C and finally to the original point B. It is clear that the sections of the trajectory corresponding to positive flow will induce velocity profiles different as the ones for negative flow since director's field will be different as well. This directional response is reflected in the average viscosity of the LC

$$\langle \eta(q,m) \rangle \equiv \int_{-1/2}^{1/2} \eta\left[\theta\left(\varsigma\right)\right] \mathrm{d}\varsigma, \tag{11}$$

where $\eta\left[\theta\left(\varsigma\right)\right]$ is the position-dependent viscosity given by eq. (6).

In fig. 7, we show the average viscosity as a function of m for the first of the trajectories described above. We observe an interesting non-Newtonian behavior with alternate regions of shear thickening and thinning. The regions of shear thinning are the result of the competition between the direction of flow that tends to orientate the molecules with a tilt in the opposite direction as the original director's configuration. The contrary is true for the shear thickening region for which the contributions of the flow adds up to that of the one the system had previously. The net result is that the molecules tend to

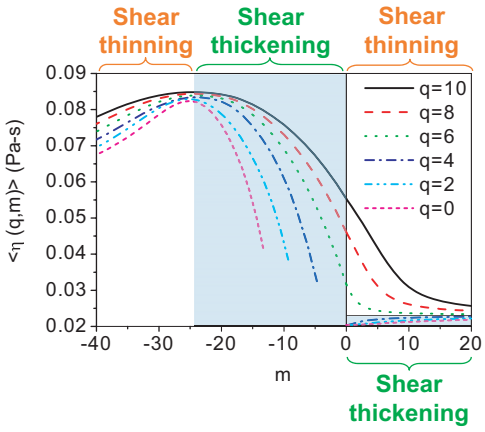

Fig. 7: Averaged apparent viscosity as a function of m showing regions of shear thickening and shear thinning.

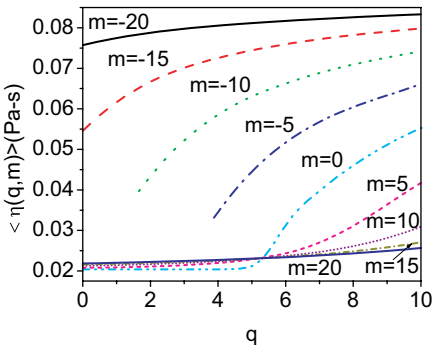

Fig. 8: Averaged apparent viscosity as a function of q showing a moderate electrorheological effect.

be more vertically aligned than in the case of zero shear. For larger magnitudes of the shear rate, the effect of the flow dominates producing the shear thinning regions. Note that the presence of the electric field renders the non-Newtonian behavior less pronounced in the sense that in this case the viscosity varies more smoothly with m. The second of the trajectories (the one starting at A' in fig. 6) would produce the same curves for the viscosity but interchanging m with $-m$.

The increase of the apparent viscosity as we increase the value of the electric field is evident in fig. 8. This electrorheological effect is of moderate intensity since the minimum value that the apparent viscosity may take is η_b, when the molecules are oriented parallel to the plates, which occurs at small shear rates and electric fields, and the maximum value that it can take is η_c, when the molecules are perpendicularly aligned with respect to the direction of flow, which occurs for large electric fields. In the present case the minimum and maximum values are $\eta_b \simeq 0.0204\,\mathrm{Pa\,s}$ and $\eta_c = 0.1052\,\mathrm{Pa\,s}$, respectively. The solutions labeled with $m < 0$ would also correspond to the second solution for the case with positive m and viceversa.

Conclusions. – In summary, based on a hydrodynamic model we have studied the flow of a homogeneous nematic

cell under the action of an applied shear flow and a perpendicular electric field. We have constructed a phase diagram in the electric field *vs.* shear rate space that shows regions in which the director's field has multiple stationary configurations. Interestingly, the selection of a given configuration of the director's field depends on the history of the sample. This may lead to a remarkable non-Newtonian behavior with alternate regions of shear thickening and thinning that may also produce an asymmetric flow profile with respect to the direction of shear by properly choosing the intensity of the electric field.

We have shown that the reorientation produced by the electric field gives rise to an augment in the apparent average viscosity of the LC as a function of the applied electric field (electrorheological effect). This viscosity can be as low as η_b and not larger than η_c. Additionally, under the action of the electric field the non-Newtonian behavior is less pronounced.

* * *

We acknowledge partial financial support from grant DGAPA-PAPIIT No. IN-107607.

REFERENCES

[1] Denniston C., Orlandini E. and Yeomans J. M., *Comput. Theor. Polym. Sci.*, **11** (2001) 389.
[2] Marenduzzo D., Orlandini E. and Yeomans J. M., *Europhys. Lett.*, **64** (2003) 406.
[3] Marenduzzo D., Orlandini E. and Yeomans J. M., *J. Chem. Phys.*, **121** (2004) 582.
[4] Rey A. D. and Denn M. D., *Annu. Rev. Fluid Mech.*, **34** (2002) 233.
[5] Han W. H. and Rey A. D., *Phys. Rev. E*, **49** (1994) 597.
[6] Toth P., Krekhov A. P., Kramer L. and Peinke J., *Europhys. Lett.*, **51** (2000) 48.
[7] Pieranski P. and Guyon E., *Commun. Phys.*, **1** (1976) 45.
[8] Vicente Alonso E., Wheeler A. A. and Sluckin T. J., *Proc. R. Soc. London, Ser. A*, **459** (2003) 195.
[9] Luskin M. and Pan T. W., *J. Non-Newtonian Fluid Mech.*, **42** (1992) 369.
[10] Zuniga I. and Leslie F. M., *Europhys. Lett.*, **9** (1989) 689.
[11] Guillén A. D. and Mendoza C. I., *J. Chem. Phys.*, **126** (2007) 204905; **127** (2007) 059901.
[12] Mendoza C. I., Corella-Madueño A. and Reyes J. A., *Phys. Rev. E*, **77** (2008) 011706.
[13] De Volder M., Yoshida K., Yokota S. and Reynaerts D., *J. Micromech. Microeng.*, **16** (2006) 612.
[14] Reyes J. A., Manero O. and Rodriguez R. F., *Rheol. Acta*, **40** (2001) 426.
[15] Rodriguez R. F., Reyes J. A. and Manero O., *J. Chem. Phys.*, **110** (1999) 8197.
[16] Negita K., *J. Chem. Phys.*, **105** (1996) 7837.
[17] Negita K., Kawano C. and Moriya K., *Phys. Rev. E*, **70** (2004) 021702.
[18] Gleeson J. T. and van Saarloos W., *Phys. Rev. A*, **44** (1991) 2588.
[19] Narumi T., See H., Yamaguchi Y. and Hasegawa T., *JSME Int. J. Ser. B* , **48** (2005) 524.
[20] Kleman M. and Lavrentovich O., *Soft Matter Physics* (Springer-Verlag, New York) 2003.
[21] Miesowicz M., *Nature*, **17** (1935) 261.
[22] Press W. H. *et al.*, *Numerical Recipes: The Art of Scientific Computing* (Cambrige University Press, Cambridge) 1986.